Journal of Oceanology and Limnology
Vol. 44, No. 3, pp. 1042-1058, 2026
https://doi.org/10.1007/s00343-025-5139-4

Research Paper

Vertical change of living siliceous radiolarians and their responses to water masses in the tropical Southeast Indian Ocean in spring*

Xiawen CHENG[1, 2, 3], Lanlan ZHANG[1, 2, **], Batagoda Gamage Dumudu Ojithma PERERA[1, 2, 3], Rong XIANG[1, 2]

[1] *State Key Laboratory of Tropical Oceanography, South China Sea Institute of Oceanology, Chinese Academy of Sciences, Guangzhou 511458, China*

[2] *Laboratory of Ocean and Marginal Sea Geology, South China Sea Institute of Oceanography, Chinese Academy of Sciences, Guangzhou 511458, China*

[3] *University of Chinese Academy of Sciences, Beijing 100049, China*

Received May 7, 2025; accepted in principle Jul. 5, 2025; accepted for publication Sep. 4, 2025

Abstract Due to scarce in-situ research, little is known about planktonic biodiversity in deep sea and their environmental characteristics. The water masses in upper 3 000 m of the tropical Southeast Indian Ocean were sampled with the Maxi Multi Plankton Sampler and the containing Radiolaria species were identified, from which the vertical spectra of the species composition were clarified. Radiolarians displayed a classic shallow subsurface abundance maximum of 1 428–1 635 inds./m^3 in 50–100 m, followed by a steep decline with increasing depth. Variance partitioning analysis indicated that temperature was the principal driver of vertical community structure, followed by silicate concentration. Nonetheless, water masses with different salinity modulated the vertical compression or expansion of radiolarian assemblages within a confined depth range. Cluster analysis and ordination analysis showed that radiolarian communities in two regions exhibited four depth-specific assemblages. In the euphotic layer, *Dictyocoryne muelleri*, *Dictyocoryne truncatum*, *Didymocrytis tetrathalamus*, *Spongaster tetras*, *Tetrapyle* spp., *Acanthodesmia vinculata*, *Botryocyrtis scutum*, and *Zygocircus microporus* were dominated and controlled by high temperature and adequate light. *Anthosphaera minuta*, *Xiphatractus* aff. *trachyphloius*, and *Anthocyrtidium zanguebaricum* were dominant species in Persian Gulf Water (200–500 m), while *Amphisphaera umbilicata*, *Spongopyle* aff. *osculosa*, *Spongotrochus vitabilis*, *Lamprotripus hirundo*, and *Sethoconus* sp. A were typical in the Red Sea Water (500–2 000 m) and could tolerate relatively lower dissolved oxygen (approx. 50 μmol/kg). The nutrient-rich Indonesian Intermediate Water could increase the growth of *Actinomma eriosperma* below 1 000 m. *Amphisphaera* aff. *xiphydrion* and *Dictyophimus platycephalus* reflecting rich silicate were probably influenced by the Circumpolar Deep Water.

Keyword: living radiolarian; depth-zonation; depth-specific water mass; tropical Southeast Indian Ocean

1 INTRODUCTION

Siliceous radiolarians, as holoplankton protists, are globally distributed and inhabit ocean water from the surface to abyssopelagic depth (Suzuki and Not, 2015) and are widely used to reconstruct the past oceanographical change. Generally, their sizes range from tens to hundreds of micrometers, and

* Supported by the National Natural Science Foundation of China (NSFC) (Nos. 42176080, 42476067), the National Key Research and Development Program of China (No. 2022-24), the Development Found of South China Sea Institute of Oceanology of Chinese Academy of Sciences (No. SCSIO202201), and the NSFC Shiptime Sharing Project (Nos. 41649910, 42149910)

** Corresponding author: llzhang@scsio.ac.cn

easily driven by hydrodynamic conditions (e.g., water mixture, ocean currents, and water masses) (Qiu et al., 2021). Radiolarians are the fundamental components of marine ecosystem, and greatly contribute to marine biogenic silica production (Lampitt et al., 2009; Zhang et al., 2015; Biard, 2022). Zasko and Rusanov (2005) indicated that the contribution of radiolarians to the total zooplankton biomass was up to 11.5% in euphotic zones. An in-situ study in the subarctic Pacific demonstrated that radiolarian contributions reached >50% of biogenic silica production in late spring to early summer (Takahashi, 1991). Diatoms are recognized as the largest global contributors to the Si cycle; however, current studies highlighted that radiolarians significantly contributed to the standing stock and production of biogenic silica on a global scale, and increased the Si output of the ocean (Maldonado et al., 2019; Llopis Monferrer et al., 2020). Therefore, it is very important to know the ecology of recent radiolarians, which would increase the paleoceanographical proxy and improve our understanding of their biogeographical distributions and biological-pump roles in the global biogeochemical cycle.

Investigations of living radiolarian distributions in the water column have predominantly focused on the euphotic zone (Renz, 1976; Dworetzky and Morley, 1987; Boltovskoy et al., 1996; Welling et al., 1996; Zasko and Rusanov, 2005; Ishitani and Takahashi, 2007; Hu et al., 2015; Boltovskoy, 2017). A few studies exceeding 1 000 m in depth have primarily been conducted in middle and high latitude regions (Itaki, 2003; Tanaka and Takahashi, 2008; Matsuzaki et al., 2020; Zhang et al., 2023) (Fig.1a).

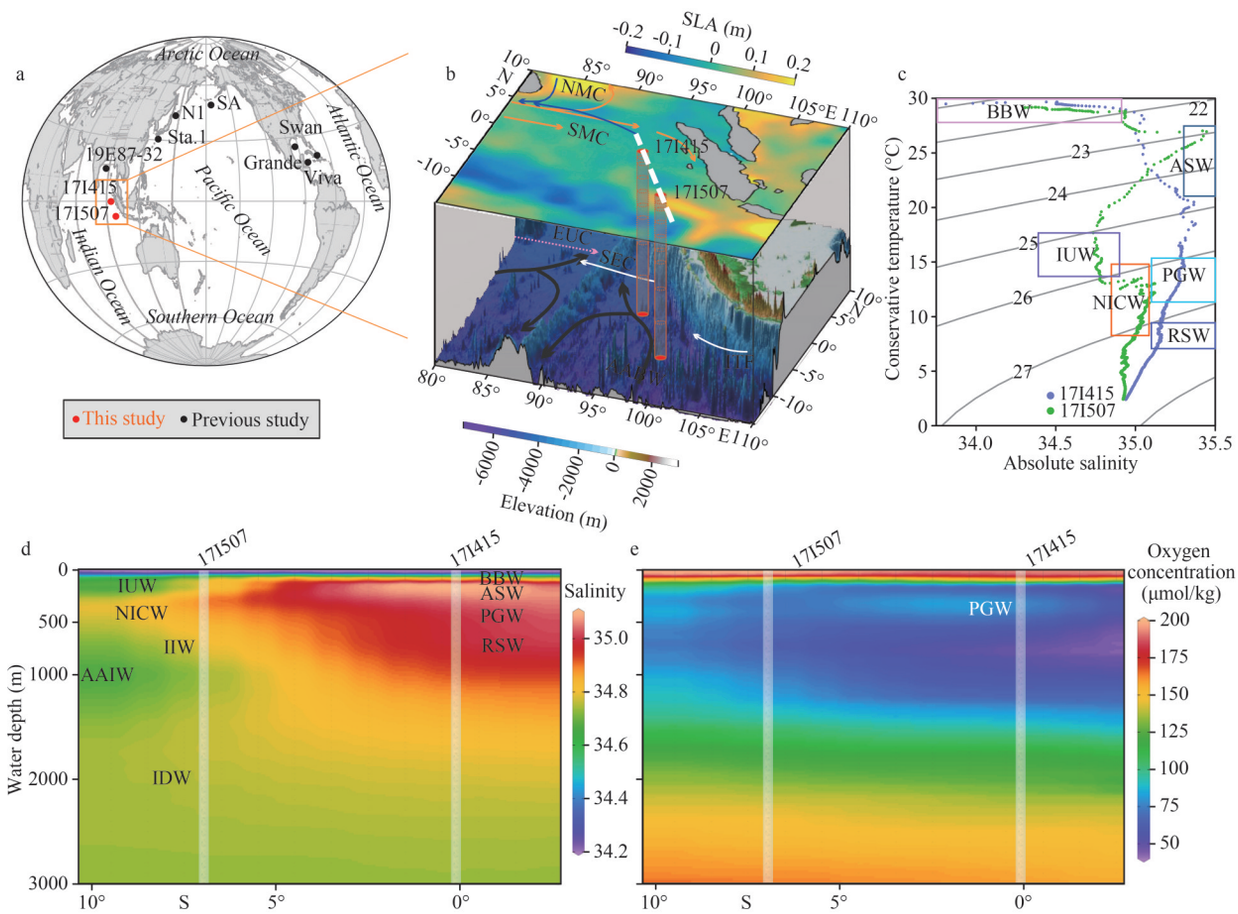

Fig.1 Study region and the hydrological environment of the sampling section

a. geographical locations of sampling stations for life research at depths exceeding 1 000 m. The information of these positions is shown in Table 1. The box means the study area; b. sampling stations, current system, and variations in monthly sea level height anomaly (SLA) averages for March 2017. SLA data were provided by Copernicus Climate Change Service (https://cds.climate.copernicus.eu); c. temperature-salinity plot of stations 17I415 and 17I507. The boxes indicate the water masses. The information of the water masses is shown in Table 2. BBW: Bay of Bengal Water; ASW: Arabian Sea Water; PGW: Persian Gulf Water; RSW: Red Sea Water; IUW: Indonesian Upper Water; NICW: North Indian Central Water; d. profiles of salinity. IIW: Indonesian Intermediate Water; AAIW: Antarctic intermediate water; IDW: Indian Deep Water; e. profiles of dissolved oxygen concentration. The section data of salinity and oxygen are annual average data provided by the WOA 2018 of the 1900–2017 period.

These studies have demonstrated that radiolarian taxa are classified into several depth-zonal groups and confined to specific water conditions. However, little is known about the knowledge of vertical change of radiolarians dwelling in deep waters, especially in tropical equatorial regions.

Based on in-situ observation, this study presents the first stratified samples and data of living radiolarian species collected throughout the 3 000-m water column from the tropical Southeast Indian Ocean (tSEIO). We investigated the vertical distribution of siliceous radiolarian species and discussed their responses to the depth-specific hydrodynamical conditions. The quantitative abundance data obtained in this study provide essential observational database for future estimates of radiolarian-contributed biosilica export fluxes.

2 MATERIAL AND METHOD

2.1 Collection of plankton tow samples

The in-situ collections of samples and data was conducted during the comprehensive expedition of the eastern Indian Ocean cruise by R/V *Shiyan 3*, operated by the South China Sea Institute of Oceanology, Chinese Academy of Sciences (CAS) in March 2017. Plankton samples were obtained at 2 stations: equartorial station 17I415 and 6.97°S station 17I507 (Fig.1a; Table 1). Station selection was designed to contrast vertical distributions of radiolarians under contrasting water mass. The equatorial station 17I415 was influenced by higher-salinity water (You, 1997), while the 6.97°S station 17I507 was located in lower-salinity water affected by Indonesian Throughflow water (Makarim et al., 2019). Nine stratified samples throughout the 3 000-m water column (0–50, 50–100, 100–200, 200–300, 300–400, 400–500, 500–1 000, 1 000–2 000, and 2 000–3 000 m) at each station were collected using a vertical Multi Plankton Sampler (type: maxi with 9 nets; micro meshes: 63 μm; company: HYDRO-BIOS KIEL, Germany). The collected plankton samples were preserved in 5% buffered formalin and stored at approximately 2 °C in a shipboard refrigerator for subsequent laboratory analysis. Chlorophyll-*a* concentration throughout the 3 000-m water column was simultaneously acquired by the chlorophyll sensors integrated into the Maxi Multi Plankton Sampler. The data of temperature and salinity were obtained using a conductivity-

Table 1 Geographical locations of all the studied stations about living radiolarians distributed in deep sea

Station	Latitude	Longitude	Sampling time	Mesh size (μm)	Sampling depth (m)	Reference
Vina	20°30′N	73°00′W	–	76	0–3 893 (6 layers)	McMillen and Casey, 1978
Swan	17°45′N	83°55′W	–	76	0–5 285 (8 layers)	McMillen and Casey, 1978
Grande	25°20′N	93°06′W	–	76	0–1 942 (6 layers)	McMillen and Casey, 1978
SA	49°00′N	174°00′W	June 2006	63	0–3 000 (15 layers)	Tanaka and Takahashi, 2008
N1	42°52′N	145°55′E	July 1999	63	0–2 000 (9 layers)	Itaki, 2003
Sta. 1	30°29′N	132°25′E	May 2015	63	0–3 000 (6 layers)	Matsuzaki et al., 2020
19E87-32	15°00′N	86°56′E	April 2019	63	0–2 600 (9 layers)	Zhang et al., 2023
17I415	0°7′S	94°13′E	March 2017	63	0–3 000 (9 layers)	This study
17I507	6°58′S	98°20′E	March 2017	63	0–3 000 (9 layers)	This study

– means the original reference does not mention the sampling time.

Table 2 The thermohaline characteristics of the water masses in the tSEIO

Water mass	Temperature range (°C)	Salinity range	σ_θ(kg/m^3)	Reference
BBW (Bay of Bengal Water)	25–29	28–35	21–23	Emery and Meincke, 1986
IUW (Indonesian Upper Water)	8–23	34.4–35	23–37	Emery and Meincke, 1986
ASW (Arabian Sea Water)	24–28	35.3–36.7	22.8–24.5	Kumar and Prasad, 1999
PGW (Persian Gulf Water)	13–19	35.1–37.9	26.2–26.8	Kumar and Prasad, 1999
RSW (Red Sea Water)	9–11	35.1–35.6	27–27.4	Kumar and Prasad, 1999
NICW (North Indian Central Water)	6–15	34.84–35.1	25.7–27.3	You and Tomczak, 1993

σ_θ means density anomaly.

temperature-depth (CTD) instrument.

Generally, a mesh size of 63 μm is used for plankton net tows in living radiolarian research (Table 1). Based on previous field sampling experience, using a smaller mesh size may underestimate the real radiolarian abundance and diversity, because the smaller mesh size would cause clogging the net during vertical tows, preventing seawater from being filtered out quickly and leading to organisms being washed out of the net. In addition, the extant radiolarian taxa possess radial spines, and plankton in seawater often aggregate into clusters, and the majority of radiolarian skeletons are larger than 63 μm. Therefore, using a 63-μm mesh size is sufficient to capture radiolarians and reflect the true community composition and species diversity.

2.2 Radiolarian processing

Following the radiolarian plankton sample processing methods, all or half of the samples were stained with Rose Bengal to distinguish the living specimens (Itaki et al., 2003; Zhang et al., 2009, 2020). Considering that the average size of radiolarians ranges from 50 to 300 μm (De Wever et al., 2001), samples in the size range of 63–500 μm were selected for slide preparation (Tanaka and Takahashi, 2008). Due to the lack of comprehensive reference material for living radiolarians, we generated an extensive photographic atlas of morphotypes encountered in this study and aligned them with current references of both living and dead siliceous/polycystine radiolarian specimens (Haeckel, 1887; Chen and Tan, 1996; Matsuzaki et al., 2020; Munir et al., 2020, 2021; Zhang et al., 2020) as the consistent identification standard for our samples. Previous studies have indicated that identifying at least 300 individuals per sample achieves a 95% confidence level for species with 1% relative abundance, while counting 500 individuals per sample increases this confidence to 99% (Lu, 1999; Qiu et al., 2024). To ensure a thorough and representative assessment of radiolarian populations, a minimum of 500 specimens from the 0–200 m must be identified. For depth greater than 200 m, where individual density decreases, the minimum required count was adjusted to 300 individuals to maintain the accuracy of radiolarian community assessment. All slides were examined and counted if the number of radiolarian specimens was less than 500 or 300.

2.3 Statistical analysis

Species with a relative abundance exceeding 2% are generally considered dominant (McNaughton, 1967). A major challenge for planktonic sampling is that the upper tows capture organisms that are actively alive, while the deeper tows collect a mix of species that genuinely inhabit those depths alongside undegraded cells that have drifted downward from the upper layers (Boltovskoy, 2017). To address this issue, a strategy involving the detection of abundance peaks within vertical profiles is employed, these peaks are often distinct within specific depth ranges, reflecting the preferred living depths of various species (Kling and Boltovskoy, 1995; Boltovskoy et al., 1996). Therefore, we selected dominant species based on the consistency between the peak depth of relative abundance and determined the absolute abundance of dominant species at the corresponding living depth. The objective is to characterize assemblages based on the relative importance of the species (Boltovskoy, 2017).

R-mode cluster analysis of the selected dominant radiolarian species was performed using SPSS 25. Detrended correspondence analysis (DCA) was initially used to check the linear or unimodal character of the species data in relative abundances at each station. The length of the first DCA axis was >4, indicating the unimodal character of the species data and canonical correlation analysis (CCA) should be performed, while the first DCA axis was <3, suggesting the linear character of the species and redundancy analysis (RDA) would more appropriate (Lepš and Šmilauer, 2003). Based on the results, CCA was appropriate for equatorial station, while RDA was more suitable for 6.97°S station to investigate the correlation between dominant radiolarian assemblages and environment parameters at water depth specific conditions. Environmental data and dominant species data were analyzed by CANOCO 5. Variance partitioning analysis (VPA) was calculated by the package “rdacca.hp” in R, and showed the contribution of each environmental parameter to the total variation in species distributions (Borcard et al., 1992). Environment parameters of oxygen, nitrate, phosphate, and silicate were provided by the World Ocean Atlas 2018 (WOA 2018) (https://www.ncei.noaa.gov/access/world-ocean-atlas-2018), based on a 1°×1° (latitude×longitude) resolution March or annual average from 1900 to 2017. The March average data were used for the upper 500 m of the water column,

given that the Indian Ocean is significantly influenced by seasonal changes. Below 500 m, annual average data were used, considering that only annual average data are available and that seasonal variations are minimal in the deep sea. The original data were interpolated to sampling stations to obtain the relevant environmental data of the corresponding stations. Since temperature and salinity data obtained by CTD only extended to 2 000 m, we combined the measured data with the WOA 2018 data to supplement the temperature and salinity from 2 000 to 3 000 m.

3 RESULT

3.1 Hydrologic condition during the sampling period

Figure 2a–c shows the vertical changes of temperature, salinity and chlorophyll-*a* concentration from surface to deep water (0–3 000 m) during our sampling periods. The sea surface temperature was high (approx. 29 °C) under the influence of the Indo-Pacific warm pool. At 6.97°S station, the warm water was deeper than that of equatorial station (Fig.3a). The surface sea salinity was relatively low (<34.5) and peaked at 100 m (35.2–35.3). Generally, then, the salinity gradually decreases. However, there significant low salinity occurred throughout the 100–200-m water column at 6.97°S station from the southern region (Fig.2b). The Deep Chlorophyll Maximum (DCM) layer at equatorial station was deeper than that at 6.97°S station (Fig.2c). At the equatorial station, the DCM layer occurred at depths of 60–100 m. In contrast, at 6.97°S station, the DCM layer was thicker ranging from 30 to 100 m (Fig.2c).

3.2 Abundance and species composition of radiolarians

Figure 2d shows the depth profiles of living radiolarian densities throughout the water column from the surface to 3 000-m depth. The highest abundance of living radiolarians in spring, off the coast of Sumatra was up to 1 635 inds./m^3 at equatorial station and 1 429 inds./m^3 at 6.97°S station respectively, both occurring within the 50–100-m depth. The abundance of 6.97°S station exceeded 1 000 inds./m^3 within the depth range of 0–100 m, whereas the abundance of equatorial station varied greatly between 0–50 m (792 inds./m^3) and 50–100 m (1 635 inds./m^3). Below 200 m, radiolarian abundance declined rapidly with increasing water depth. At about 500 m, the abundance dropped to single digits, and at 2 000–3 000 m the abundance was about 0.1 inds./m^3. Although the abundance of radiolarians in the 2 000–3 000-m depth range appeared low, the number of individuals captured still reached 77–152.

A total of 334 distinct radiolarian species at equatorial station and 308 radiolarian species at 6.97°S station were identified. The dominant species were presented in Plates 1–2. The species

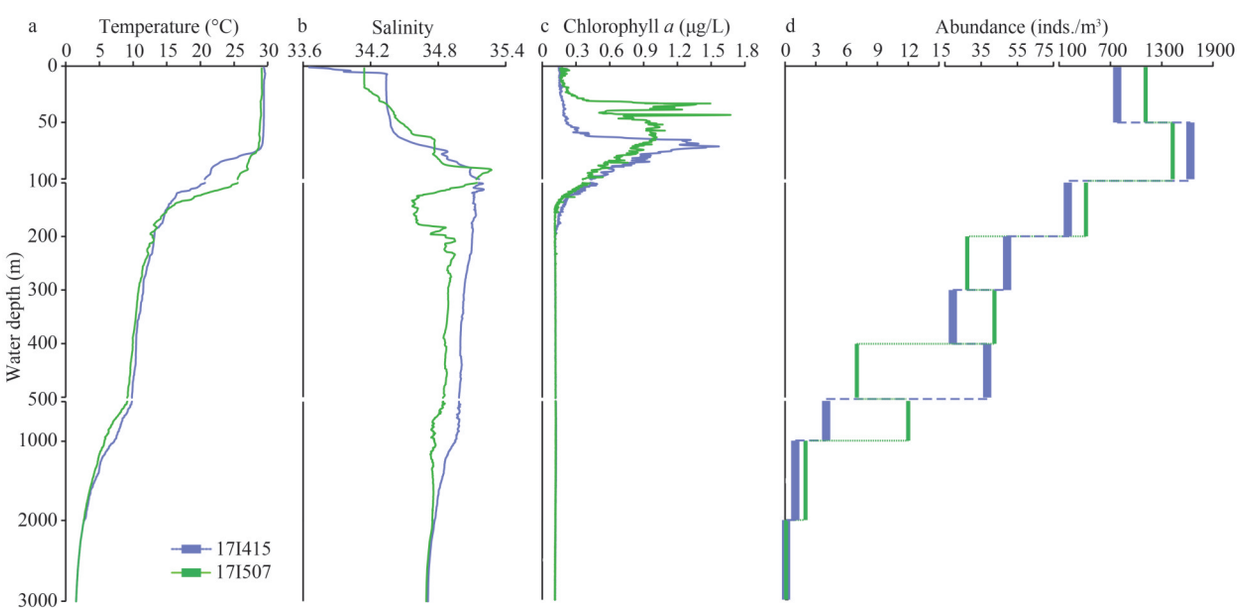

Fig.2 Vertical changes of in-situ hydrological parameters and living radiolarian abundances with water depth at stations 17I415 and 17I507

a. temperature; b. salinity; c. chlorophyll-*a* concentration; d. living radiolarian abundance.

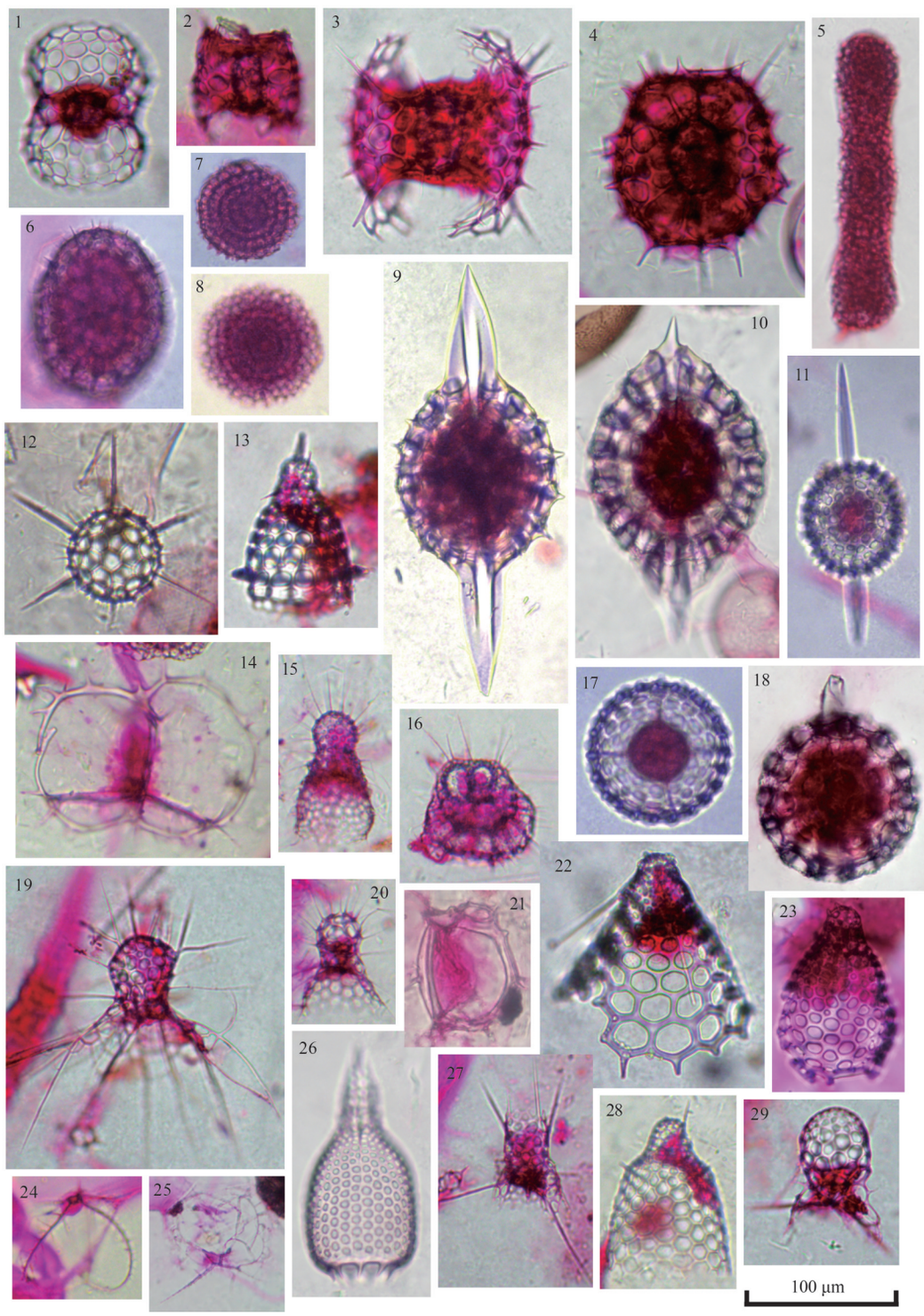

Plate 1 Dominant radiolarian species in this study (1)

1. *Didymocrytis tetrathalamus* Haeckel; 2. *Tetrapyle* spp.; 3. *Tetrapyle octacantha* Müller; 4. *Phorticium polycladum* Tan and Tchang; 5. *Spongurus cylindricus* Haeckel; 6. *Larcopyle buetschlii buetschlii* Zhang and Suzuki; 7. *Flustrella heterocyclus* (Haeckel); 8. *Flustrella perispira* (Haeckel); 9. *Amphisphaera* aff. *xiphydrion* (Chen); 10. *Amphisphaera umbilicata* (Dreyer); 11. *Druppatractus hastatus* Blueford; 12. *Acanthosphaera minuta* Cleve; 13. *Diplocyclas bicorona* Haeckel; 14. *Acanthodesmia vinculata* Müller; 15. *Dictyocryphalus hispidus* Ehrenberg; 16. *Botryocyrtis scutum* (Harting); 17. *Thecosphaera zittelii* Dreyer; 18. *Xiphatractus* aff. *trachyphloius* Chen and Tan; 19. *Archiperidium circumtexta* (Haeckel); 20. *Dictyocryphalus democriti* (Haeckel); 21. *Zygocircus micropora* (Popofsky); 22. *Sethoconus* sp. A; 23. *Lamprocyrtis heteroporos* (Hays); 24. *Neosemantis distephanus* (Haeckel); 25. *Plectacantha trichoides* Jörgensen; 26. *Anthocyrtidium zanguebaricum* (Ehrenberg); 27. *Amphiplecta* sp. A; 28. *Sethoconus* aff. *tabulata* (Ehrenberg); 29. *Archiperidium hexacantha* (Popofsky).

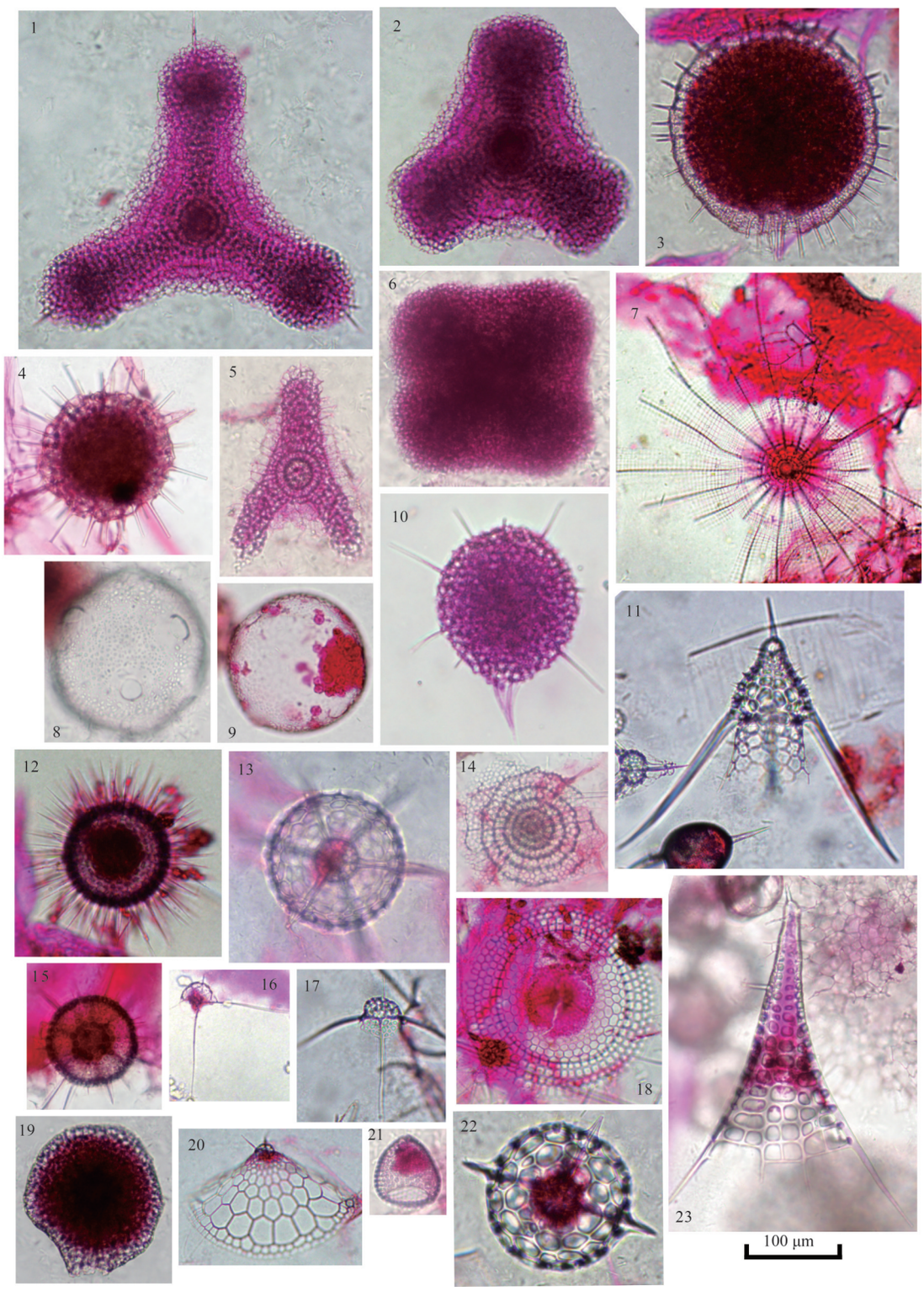

Plate 2 Dominant radiolarian species in this study (2)

1. *Dictyocoryne profunda* Ehrenberg; 2. *Dictyocoryne truncatum* (Ehrenberg); 3. *Spongotrochus glacialis* Poplfsky; 4. *Spongotrochus vitabilis* Goll and Bjørklund; 5. *Dictyocoryne muelleri* (Haeckel); 6. *Spongaster tetras* Ehrenberg; 7. *Litharachnium tentorium* Haeckel; 8–9. *Collosphaera brachysiphonia* (Dumitrica); 10. *Spongodiscus helioides* (Cleve); 11. *Lamprotripus hirundo* (Haeckel); 12. *Thecosphaera multispinula* (Su); 13. *Hexacantium hexagonale* Haeckel; 14. *Stylochlamydium asteriscus* Haeckel; 15. *Actinomma eriosperma* Tan; 16–17. *Dictyophimus platycephalus* Haeckel; 18. *Eucecryphalus tricostatum* (Haeckel); 19. *Spongopyle* aff. *osculosa* Dreyer; 20. *Clathrocyclas danaoes* Haeckel; 21. *Carpocanium obliqua* (Haeckel); 22. *Hexacontium gracilenta* (Chen and Tan); 23. *Polypleuris pyrgina* Sugiyama.

Dictyocoryne muelleri, *Dictyocoryne truncatum*, *Didymocrytis tetrathalamus*, *Spongaster tetras*, *Tetrapyle* spp., *Acanthodesmia vinculata*, *Botryocyrtis scutum*, *Neosemantis distephanus*, and *Zygocircus microporus* were dominant in 0–100 m at both stations. In addition to the shared species in 0–100 m, *Collosphaera brachysiphonia*, *Phorticium polycladum*, and *Spongodiscus helioides* were dominant in 0–200 m at the 6.97°S station. *Larcopyle buetschlii buetschlii*, *Stylochlamydium asteriscus*, and *Sethoconus* aff. *tabulata* were primarily distributed in 100–300 m at the equatorial station. *Anthosphaera minuta*, *Thecosphaera multispinula*, *Xiphatractus* aff. *trachyphloius*, *Anthocyrtidium zanguebaricum*, and *Diplocyclas bicorona* were dominant in 200–500 m. Among them, *T. multispinula* and *D. bicorona* were also dominant in 200–1 000 m at the 6.97°S station. *Amphisphaera umbilicata*, *Spongopyle* aff. *osculosa*, *Spongotrochus vitabilis*, *Lamprotripus hirundo*, and *Sethoconus* sp. A were dominant in 500–2 000 m at the equatorial station. *Actinomma eriosperma* was dominant in 1 000–2 000 m at the 6.97°S station. *Amphisphaera* aff. *xiphydrion* and *Dictyophimus platycephalus* were dominant in 2 000–3 000 m at both stations.

3.3 Statistical analysis

In order to have a better understanding of how radiolarian assemblages vary with water depth, different combinations were obtained by cluster analysis. The samples from equatorial station were classified into 4 groups representing radiolarian communities adapted to depth specific environments: group A (shallow assemblage, 0–100 m), group B (intermediate assemblage, 100–500 m), group C (intermediate-deep assemblage, 500–2 000 m) and group D (deep assemblage, 2 000–3 000 m) (Fig.3a). Similarly, at 6.97°S station, the samples were categorized into 4 groups: group I (shallow assemblage, 0–200 m), group II (intermediate assemblage, 200–1 000 m), group III (intermediate-deep assemblage, 1 000–2 000 m), and group IV (deep assemblage, 2 000–3 000 m) (Fig.4a). The species composition for each group is illustrated in Figs.3b & 4b.

Ordination analysis was conducted to investigate the relationship between environmental factors and radiolarian species. As mentioned in the Materials and Methods section, CCA was used for equatorial station and RDA was used for 6.97°S station. Results show that radiolarian composition at both stations was affected by the environmental factors.

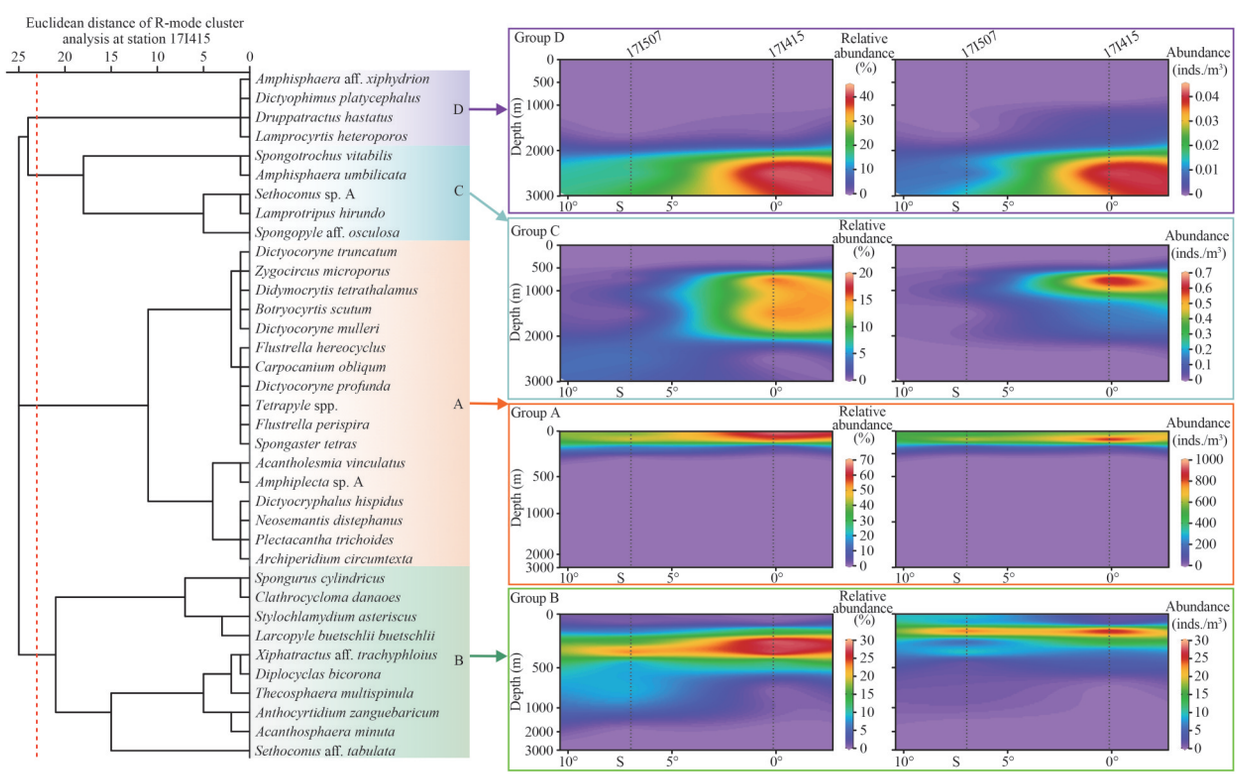

Fig.3 Results of the R-mode cluster analysis based on the relative abundances of dominant species at station 17I415

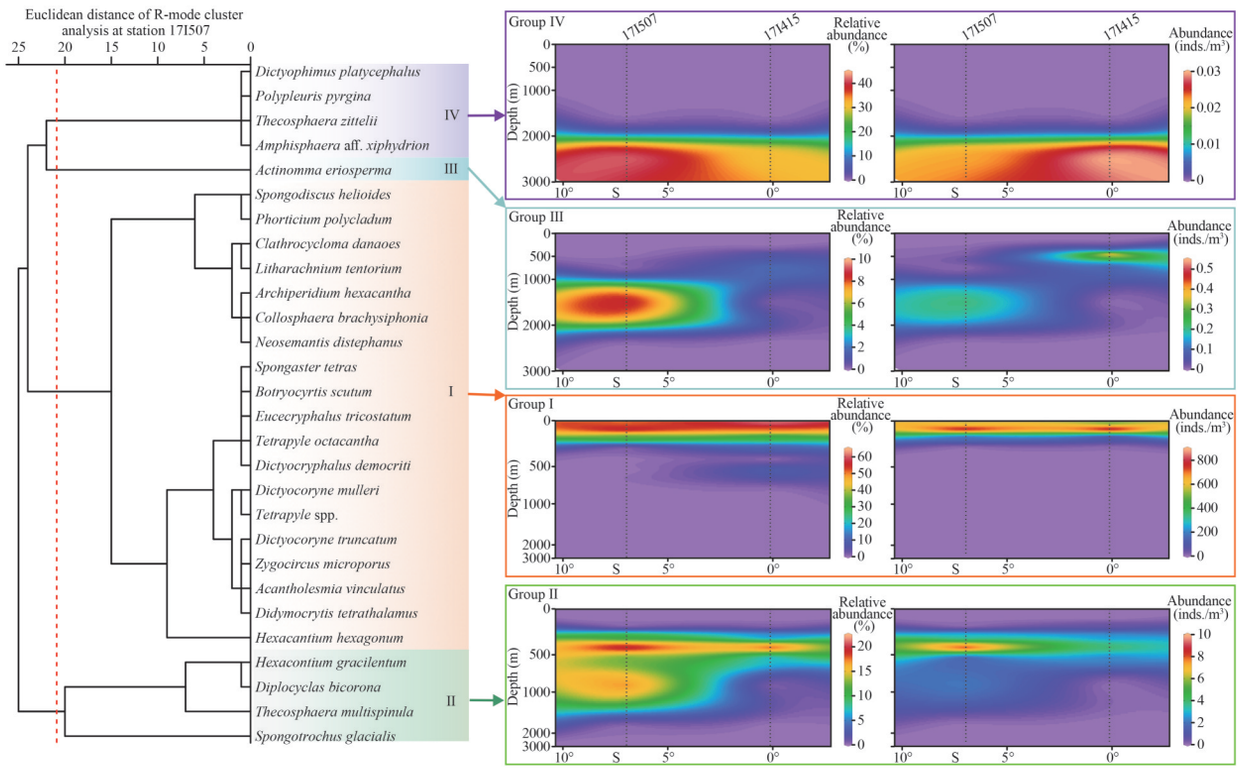

Fig.4 Results of the R-mode cluster analysis based on the relative abundances of dominant species at station 17I507

A total of 44.41% of cumulative variance in species was explained by the first two axis at equatorial station and 66.31% at 6.97°S station. Temperature and chlorophyll-*a* concentration were the most significant explanatory factors for group A and group I. In contrast, salinity was the primary explanatory factors for group B and group II. At deeper layers, nutrients, particularly silicates, contribute to community composition, notably influencing the assemblages in group D and group IV (Fig.5).

VPA revealed the differences in the independent contributions of the environmental variables (Fig.6). Temperature exhibited the largest independent effect (29.85%, $P<0.01$), followed by silicate (28.47%, $P<0.01$), phosphate (27.45%, $P<0.05$) and dissolved oxygen (22.77%, $P<0.05$). In contrast, salinity (-3.14%) and chlorophyll *a* (-5.55%) returned negative values.

4 DISCUSSION

4.1 Regional characteristic of living radiolarians and influencing factors

Our data firstly presented the depth distributions of living radiolarians from surface to the deep sea in the tSEIO. The abundance of radiolarians throughout the entire water column was 2 731–3 055 inds./m^3 during spring—the inter-monsoon transition—typically a season of lower biological productivity compared with monsoon periods (Priyanka et al., 2025). And the radiolarians exhibited a classic shallow subsurface abundance maximum. The abundance increased from 780–1 113 inds./m^3 in the 0–50-m layer to a pronounced peak of 1 428–1 635 inds./m^3 at 50–100 m. The depth of the abundance maximum in the tSEIO was consistent with that reported for other oceanic regions, occurring at approximately 50–100 m. However, the magnitude of the peak in the tropical zone was markedly higher than in temperate and high-latitude waters (Abelmann and Gowing, 1996; Ikenoue et al., 2019, Okazaki et al., 2004); reflecting the efficient utilization of scarce nutrients by radiolarians in oligotrophic tropical waters and the stimulatory effect of higher temperatures on growth (Anderson et al., 1989). In tropical and subtropical regions, the peak abundance of the tSEIO was comparable to the standing stock of nutrient-rich semi-enclosed marginal seas such as the Japan Sea (a maximum of 1 574 inds./m^3) and the South China Sea (a maximum of 3 339 inds./m^3) (Ishitani and Takahashi, 2007; Hu et al., 2015). While in the marginal seas of the Atlantic Ocean

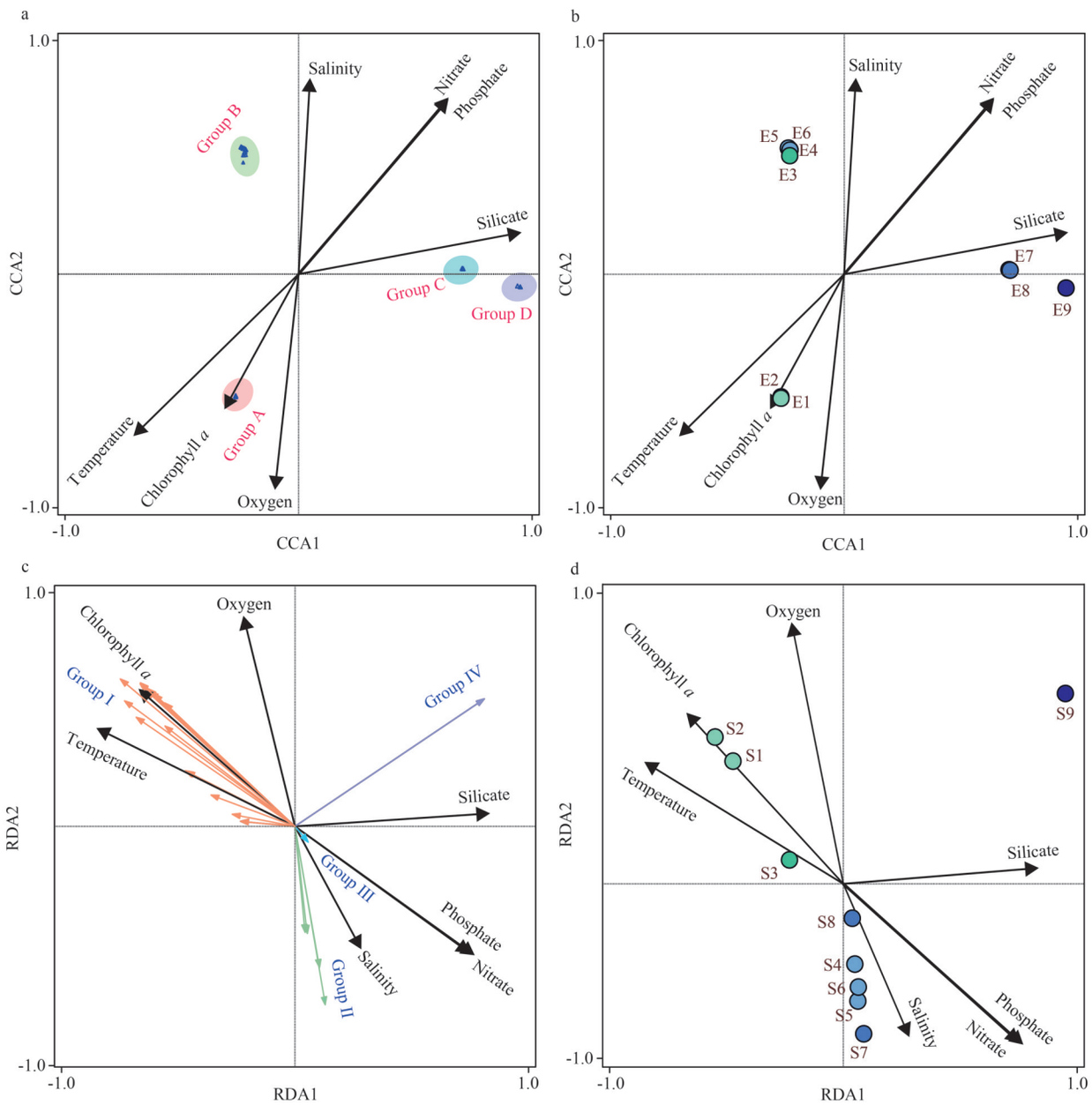

Fig.5 The sequence diagram of the ordination analysis of dominant radiolarian species and environmental parameters

a, c. sequence diagram of species and environmental variables, for equatorial station (group A–D) and 6.97°S station (group I–IV); b, d. sequence diagram of samples and environmental variables. E1–E9 means water layers from 0–50 to 2 000–3 000 m in equatorial station, and S1–S9 means water layers from 0–50 to 2 000–3 000 m in 6.97°S station.

(the Gulf of Mexico and the Caribbean Sea), radiolarian abundance was limited to a maximum of 150 inds./m^3 (McMillen and Casey, 1978). Below the peak, the abundance dropped to 201–414 inds./m^3 at 100–200 m, declined sharply to approximately 10 inds./m^3 at 500–1 000 m in the tSEIO, which was comparable to those currently reported for the North Pacific, Arctic Ocean, and Southern Ocean (Abelmann and Gowing, 1996; Okazaki et al., 2004; Ikenoue et al., 2015; Matsuzaki et al., 2016). Unlike the subarctic Pacific and the northern Japan Sea, where abundances exceeded 10 individuals inds./m^3 even at 1 000–3 000 m (Itaki, 2003; Tanaka and Takahashi, 2008), these depths in the tSEIO were few. The vertical attenuation of tSEIO was markedly steeper.

Although radiolarian abundances were generally high throughout the tSEIO, the spatial heterogeneity existed between the two stations, reflecting the influence of local hydrographic conditions. Unlike equatorial station, which showed a significant gap in

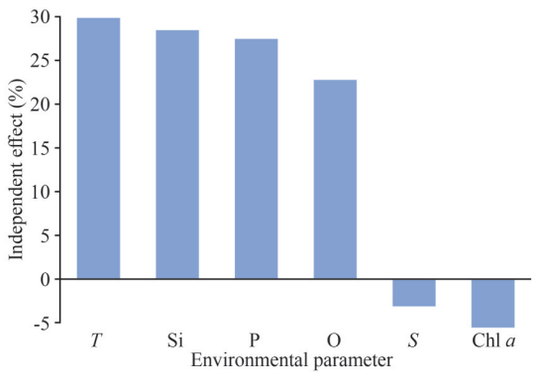

Fig.6 The independent effects of environmental parameters to radiolarian community structure revealed by variance partitioning analysis

T: temperature; Si: silicate; P: phosphate; O: oxygen; *S*: salinity; Chl *a*: chlorophyll *a*.

abundance between the 0–50- and 50–100-m layers, 6.97°S station had an abundance exceeding 1 000 inds./m^3 in both layers (Fig.2d). This pattern may correlate well with the thicker DCM layer at 6.97°S station. The positive sea level height anomaly at 6.97°S station (Fig.1b) indicated the presence of an anticyclonic eddy, characterized by the downward extension of warm water and a deeper mixed layer (Gaube et al., 2019), as evidenced by the vertical temperature profile (Fig.2a). The relative stability of the water column restricted vertical mixing in the anticyclonic eddy region (He et al., 2020), contributing to the flourishing of Collodaria at 6.97°S station. Feng et al. (2024) pointed that regions influenced by anticyclonic eddies exhibited a steady increase in dinoflagellate abundance and a significant decline in diatoms as temperatures rose. Dinoflagellates form symbiotic associations with several shallow-dwelling radiolarian species (Zhang et al., 2018), whereas diatoms and radiolarians compete for dissolved silicate during the formation of siliceous frustules or skeletons (Lazarus et al., 2009). Consequently, the combined effect of high chlorophyll concentration and anticyclonic eddies promoted the radiolarian abundance in the euphotic layer.

Based on the results of the cluster analysis, there were four depth-zonation of living radiolarian assemblages (shallow, intermediate, intermediate-deep, and deep) in the tSEIO. The result of VPA attributed most of this vertical structuring to temperature, which exhibited the largest independent effect value (Fig.6), consistent with its overarching influence on other zooplankton assemblages (Cheng et al., 2022). The tropical submergence phenomenon, where species inhabit shallower layers at high latitudes and sink to greater depths in low latitudes (Ishitani and Takahashi, 2007), further demonstrates the decisive role of temperature in determining the depth-specific distribution of individual species. This phenomenon was observed here by *Spongotrochus glacialis*, which was restricted to 500–1 000 m in our study but occurred markedly shallower at high latitudes (Ishitani and Takahashi, 2007; Boltovskoy, 2017). Silicate contributed the second-largest independent effect value, highlighting the sensitivity of siliceous taxa to Si availability. Phosphate and dissolved oxygen also contributed positively, whereas salinity and chlorophyll *a* associations with community composition are mediated by covarying factors rather than by direct and independent drivers.

However, the living depth of the four assemblages varied between the two stations. The shallow assemblages were primarily found in 0–100 m at equatorial station but extended to 200 m at 6.97°S station. This discrepancy was attributed to the distinct water masses with different salinity influencing each depth range (Fig.5b, d). At both stations, 0–100 m was occupied by low-salinity Bay of Bengal Water (BBW) originating in the northern Bay of Bengal (Han and McCreary, 2001; Schott and McCreary, 2001). Between 100 and 200 m, the equatorial station was underlain by high-salinity Arabian Sea Water (ASW) (Schott and McCreary, 2001; Jain et al., 2017), whereas 6.97°S was ventilated by the Indonesian Throughflow (ITF) (You and Tomczak, 1993). ITF has two cores in the Indian Ocean: a salinity minimum in the upper 300 m (Indonesian Upper Water, IUW) and a deeper core of low salinity and high silica (Indonesian Intermediate Water, IIW) (Makarim et al., 2019). The shared low-salinity characteristics of the IUW and BBW in the euphotic zone explained the extended distribution of the shallow assemblages to 200 m at 6.97°S station. Similarly, the transition from intermediate to intermediate-deep assemblages occurred at 500 m at the equatorial station but reached 1 000 m at the 6.97°S station. The difference arose because the equatorial station was influenced by two distinct high-salinity water masses, Persian Gulf Water (PGW) and Red Sea Water (RSW), whereas the 6.97°S station was uniformly affected by North Indian Central Water (NICW) until 1 000 m, where IIW intruded (Fig.1d).

The results indicate that although salinity exerted no significant independent effect on community composition, its combined action with other factors delineated the depth boundaries of species distributions in the tSEIO. Regional water mass blending modulated the vertical compression or expansion of radiolarian communities within a certain range. Comparable depth-zonation patterns were documented for radiolarians in other regions, yet the specific depth ranges of shallow, intermediate, and deep assemblages varied among basins (Itaki, 2003; Matsuzaki et al., 2020), presumably reflecting regional differences in the environmental parameters of particular water layers.

4.2 Depth-zonation of living radiolarians impacted by depth specific conditions

4.2.1 Shallow assemblage controlled by high temperature and adequate light

Observations have revealed variability in radiolarian communities, which were influenced by hydrological characteristics. The study area is situated within the warm pool, characterized by permanent high surface temperature (De Deckker, 2016). *D. muelleri*, *D. truncatum*, *D. tetrathalamus*, *S. tetras*, *Tetrapyle* spp, *A. vinculata*, *B. scutum*, and *Z. microporus* were found both in group A and group I (Figs.3–4), and were identified as tropical surface water species. The composition of the shallow water assemblage in 0–100 m exhibited consistency, demonstrating uniformity in species composition in surface waters of tSEIO. Previous research has indicated that *D. truncatum*, *D. tetrathalamus*, *Tetrapyle* spp., and *S. tetras* were dominant in tropical and subtropical warm waters like the Gulf of Mexico and Caribbean, even occurred at higher latitudes in the central North Pacific influenced by Kuroshio Current (McMillen and Casey, 1978; Kling, 1979). These species are believed to be influenced by the warm and saline Kuroshio Surface Water in Pacific Ocean (Chang et al., 2003; Zhang et al., 2009; Matsuzaki et al., 2016). However, in the tSEIO, low-salinity BBW is prevalent in the upper 200 m (Jensen, 2003). This observation suggested that temperature was a more significant driver of shallow species distribution than salinity in the equatorial ocean. Culture experiments on *D. truncatum* also demonstrated that the species exhibited a wide tolerance for variations in salinity (27–35) (Matsuoka and Anderson, 1992). In the tSEIO, these species were flourishing in the water temperature of 20.69–29.43 °C and salinity of 33.65–35.16.

Previous epifluorescence staining has confirmed that these species all harbor photosynthetic symbionts (Zhang et al., 2018), which impose a light requirement and restrict their vertical distribution to the euphotic zone. These species accounted for 32%–54% collectively of the water-column abundance, and their dominance drove the pronounced subsurface radiolarian peak observed in the tSEIO. Consequently, the requirement for high temperatures and adequate light are pivotal to their presence in the surface waters of the tSEIO, whereas the ability to thrive across fluctuating salinities underscored an ecological plasticity that allowed them to capitalize on widely varying environmental conditions.

4.2.2 Intermediate assemblage preferring high-salinity water masses

Below the BBW, the intermediate assemblages of radiolarians in this area were significantly influenced by salinity gradients (Fig.5). *T. multispinula* and *D. bicorona* occurred in both group B and group II (Figs.3–4), correlating with high-salinity water. In this study area, the NICW, an aged form of Indian Central Water occupies the majority of thermocline in the north Indian Ocean south of 10°S. During its transit to the northeastern Indian Ocean, NICW accumulated macronutrients while becoming depleted in oxygen (You and Tomczak, 1993; Grand et al., 2015). *T. multispinula* was one of the dominant species in the 200–500-m water column in the Pacific Ocean, characterizing the North Pacific Subtropical Mode Water (Matsuzaki et al., 2020), while *D. bicorona* was recognized as a cosmopolitan high-latitude species (Lombari and Lazarus, 1988). It can be inferred that water masses rich in *T. multispinula* and *D. bicorona* exhibit characteristics of relatively low temperature (5.78–13.17 °C), high salinity (34.77–35.11), and typically homogeneous physical properties in the vertical direction.

In the equator, the high-salinity water masses originating from the North Indian Ocean include ASW, PGW, and RSW. PGW is a high-salinity water mass found at an average depth of 200 m, with occurrences at depths of 300–400 m in the Bay of Bengal and south of the equator (Rochford, 1964). RSW is typically found at depths ranging from 500 to 1 000 m and is characterized by a weakly developed salinity maximum and low oxygen concentrations (Rochford, 1964; Kumar and Prasad,

1999). Both PGW and RSW result from excess evaporation over precipitation and are always combined into a single source of high-salinity water (You and Tomczak, 1993; Rixen and Ittekkot, 2005). However, the biological responses show differences. The PGW core layer (300–400 m) was dominated by *A. minuta*, *Xiphatractus* aff. *trachyphloius*, and *A. zanguebaricum*, whereas RSW-associated depths exhibited distinct assemblages characterized by *A. umbilicata*, *Spongopyle* aff. *osculosa*, *S. vitabilis*, *L. hirundo*, and *Sethoconus* sp. A. The evidence supported the presence of both PGW and RSW in the Bay of Bengal (Jain et al., 2017). Our study further demonstrated that taxa exhibited significantly different species responses to PGW and RSW from a biological perspective. Notably, a weak oxygen peak observed within the oxygen minimum zone in the bay at a depth of 250–400 m is associated with PGW (Jain et al., 2017), as shown in the dissolved oxygen profile (Fig.1e). The presence of *A. minuta*, *Xiphatractus* aff. *trachyphloius*, and *A. zanguebaricum* indicated that these species were well-adapted to low temperature (9.84–13.17 °C), high-salinity environment (34.99–35.11) and exhibited sensitivity to the ventilation of intermediate water. PGW brings oxygen to the Bay of Bengal to ventilate the oxygen minimum zone and contributes to the ecological functioning of this area (Sheehan et al., 2020). This is important because the northern Indian Ocean does not have its own subtropical convergence, and its thermocline water has to be replenished from the tropics and further south. Meanwhile, *Spongopyle* aff. *osculosa*, *S. vitabilis*, *L. hirundo*, and *Sethoconus* sp. A also adapted to low temperature (2.88–9.84 °C), and showed tolerance to relatively high salinity (34.78–34.99) and low oxygen conditions (approx. 50 μmol/kg). Relevant reports on these species remain scarce. In the core of Norwegian Sea, rare or trace specimens of *S. vitabilis* have been found and named (Goll and Bjørklund, 1989). *L. hirundo* was the most dominant species in the lower Sea of Okhotsk Intermediate Water, between 500 and 1 000 m (Abelmann and Nimmergut, 2005), a depth range consistent with its distribution in the tSEIO. At this depth, the salinity of the Okhotsk Seawater ranges from 33.86 to 34.38, and dissolved oxygen concentrations range from 47 to 109 μmol/kg (Yasuda et al., 2002). The findings suggested that *L. hirundo* and related species (*Spongopyle* aff. *osculosa*, *S. vitabilis*, and *Sethoconus* sp. A) may be widely distributed within this depth layer and exhibit a certain tolerance to variations in both salinity and dissolved oxygen levels, and their exact oxygen tolerance limits necessitate additional research.

4.2.3 Intermediate-deep and deep assemblage associated with nutrient water masses

The salinity minimum at 1 000 m in the tropical Indian Ocean (Fig.1d) is distinct from the salinity minimum associated with the Antarctic Intermediate Water (AAIW) in the Indian Ocean, which is referred to as IIW to denote its Pacific and Indonesian origins. The AAIW is primarily located south of 20°S, where it shifts upward to lower densities within the tropical latitudes of the IIW (Talley and Sprintall, 2005). The IIW is characterized by low-salinity and silica-rich water in the deeper core of the ITF (Talley and Sprintall, 2005; Iskandar and Suga, 2022). The ITF played a pivotal role in transporting substantial amounts of nitrate, phosphate, and silicate to the Indian Ocean (Ayers et al., 2014). Although the water masses were not identified on the *T-S* diagram at the two sampling stations, the significant concentrations of nitrates, phosphates, and silicates transported to tSEIO facilitated the proliferation of *A. eriosperma* with temperature of 2.73–5.78 °C and salinity of 34.75–34.77.

As the Indian Ocean is landlocked to the north, the Indian Ocean deep water, consisting of Circumpolar Deep Water (CDW) and Antarctic Bottom Water (AABW), are sourced from the Southern Ocean (Wyrtki, 1973). Overlying the northward transport of AABW and CDW is a southward return flow of Indian Deep Water (IDW, between 2 000 and 4 000 m) (Sloyan, 2006). The IDW presumably is generated by deep upwelling from the CDW. This water mass is characterized by low oxygen levels (<190 μmol/kg) and high salinity, resulting from its mixing with older intermediate waters above, it is also enriched in silica due to discharges from northern rivers (silicate>100 μmol/kg) (Schott and McCreary, 2001). The presence of *Amphisphaera* aff. *xiphydrion* and *D. platycephalus*, both found in the group D and group IV, which dominated the 2 000–3 000-m depth range with temperature of 1.54–2.88 °C and salinity of 34.70–34.75. They associated with silicate and may indicate the Antarctic origin.

In conclusion, the distribution and dominance of radiolarian species in the study area highlight the interactions between oceanographic water masses

and the ecological responses of marine microorganisms. The characteristics of the water masses at the two tSEIO stations and their influence on community composition were elucidated (Fig.7). The findings identify potential radiolarian indicator species associated with different water masses at varying depths, which are essential for reconstructing the evolution of paleoceanographic conditions. For instance, benthic foraminifera have been utilized to reflect the changes of deep-sea circulation in the eastern Indian Ocean during the Miocene (Verma et al., 2013). Understanding the impacts of water masses at different depths on radiolarian community structure is expected to provide insights for the reconstruction of full-depth water masses in the tSEIO throughout geological history. Although this study primarily focused on the species composition of radiolarians across different depth layers and their responses to environmental gradients, several limitations should be acknowledged. First, due to the constraints of cruise time and sampling conditions, the number of sampling stations in this study was limited, which may have led to an underestimation of radiolarian species diversity in the study area. As a result, the findings may not fully represent the ecological characteristics of the entire equatorial southeast Indian Ocean. Future studies should be incorporate multi-year continuous observations to improve data representativeness and enhance the generalizability of conclusions.

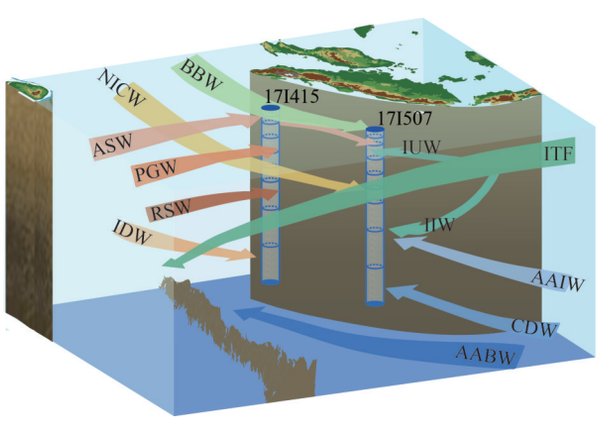

Fig.7 Schematic view of the influence of water masses on biology

BBW: Bay of Bengal Water; NICW: North Indian Central Water; ASW: Arabian Sea Water; PGW: Persian Gulf Water; RSW: Red Sea Water; ITF: Indonesian Throughflow; IUW: Indonesian Upper Water; IIW: Indonesian Intermediate Water; AAIW: Antarctic Intermediate Water; CDW: Circumpolar Deep Water; IDW: Indian Deep Water; AABW: Antarctic Bottom Water.

5 CONCLUSION

The in-situ research focused on the global equatorial deep regions are very limited yet. Using Maxi Multi Plankton Sampler, we firstly obtained the data of continuous stratified plankton samples from surface to 3 000-m depth of the tSEIO. This study analyzed the deep distribution of siliceous radiolarians and their correlations with specific conditions.

High species diversity and abundant siliceous radiolarians were observed in the equatorial and at 6.97°S regions from the tSEIO in spring. Radiolarians displayed a pronounced subsurface abundance maximum of 1 428–1 635 inds./m^3. The combined effect of high chlorophyll concentration and anticyclonic eddies promoted the radiolarian abundance in the euphotic layer. Below the peak, the abundance declined sharply. The vertical patterns of radiolarian community structure at depths of 0–3 000 m are significantly determined by temperature and silicate, resulting in four depth-zonation of living radiolarian assemblages (shallow, intermediate, intermediate-deep, and deep). However, the living depth of the four assemblages varied because salinity-defined regional water masses compress or expand radiolarian distributional boundaries within a limited depth range.

The shallow assemblages *D. muelleri*, *D. truncatum*, *D. tetrathalamus*, *S. tetras*, *Tetrapyle* spp., *A. vinculata*, *B. scutum*, and *Z. microporus* were controlled by high temperature and adequate light. The intermediate assemblages *T. multispinula* and *D. bicorona* were significantly influenced by high salinity. In addition, *A. minuta*, *Xiphatractus* aff. *trachyphloius*, and *A. zanguebaricum* were dominant in the depth influenced by PGW, whereas *A. umbilicata*, *Spongopyle* aff. *osculosa*, *S. vitabilis*, *L. hirundo*, and *Sethoconus* sp. A were characterized in the depth affected by RSW. These RSW-associated species were likely to tolerate relatively lower dissolved oxygen concentrations (approx. 50 μmol/kg). The nutrient-rich IIW can increase the growth of *A. eriosperma* below 1 000 m in the 6.97°S region. Deep assemblages *Amphisphaera* aff. *xiphydrion* and *D. platycephalus*, which reflected rich silicate, and were probably influenced by the CDW.

6 DATA AVAILABILITY STATEMENT

The datasets generated and/or analyzed during

the current study are available from the corresponding author on reasonable request.

7 ACKNOWLEDGMENT

Data and samples were collected onboard R/Vs *Shiyan 3* and *Shiyan 6* implementing the open research cruise NORC2017-10, NORC2022-10+ NORC2022-303. We gratefully acknowledge the support of the China-Sri Lanka Joint Center for Education and Research, Chinese Academy of Sciences. We are grateful to the editors and the reviewers for their valuable comments and constructive suggestions on the manuscript. We thank Prof. Gengxin CHEN from the South China Sea Institute of Oceanology, CAS, for his help with fitting the temperature and salinity data of 2 000–3 000 m, and Dr. Xu AN from the Institute of Oceanology, CAS, for her help with visualization of SLA diagram.

References

Abelmann A, Gowing M M. 1996. Horizontal and vertical distribution pattern of living radiolarians along a transect from the Southern Ocean to the South Atlantic subtropical region. *Deep Sea Research Part I*: *Oceanographic Research Papers*, **43**(3): 361-382, https://doi.org/10.1016/0967-0637(96)00003-9.

Abelmann A, Nimmergut A. 2005. Radiolarians in the Sea of Okhotsk and their ecological implication for paleoenvironmental reconstructions. *Deep Sea Research Part II*: *Topical Studies in Oceanography*, **52**(16-18): 2302-2331, https://doi.org/10.1016/j.dsr2.2005.07.009.

Anderson O R, Bennett P, Bryan M. 1989. Experimental and observational studies of radiolarian physiological ecology: 3. Effects of temperature, salinity and light intensity on the growth and survival of *Spongaster tetras tetras* maintained in laboratory culture. *Marine Micropaleontology*, **14**(4): 275-282, https://doi.org/10.1016/0377-8398(89)90014-5.

Ayers J M, Strutton P G, Coles V J et al. 2014. Indonesian throughflow nutrient fluxes and their potential impact on Indian Ocean productivity. *Geophysical Research Letters*, **41**(14): 5060-5067, https://doi.org/10.1002/2014GL060593.

Biard T. 2022. Diversity and ecology of Radiolaria in modern oceans. *Environmental Microbiology*, **24**(5): 2179-2200, https://doi.org/10.1111/1462-2920.16004.

Boltovskoy D. 2017. Vertical distribution patterns of Radiolaria polycystina (protista) in the World Ocean: living ranges, isothermal submersion and settling shells. *Journal of Plankton Research*, **39**(2): 330-349, https://doi.org/10.1093/plankt/fbx003.

Boltovskoy D, Oberhänsli H, Wefer G. 1996. Radiolarian assemblages in the eastern tropical Atlantic: patterns in the plankton and in sediment trap samples. *Journal of Marine Systems*, **8**(1-2): 31-51, https://doi.org/10.1016/0924-7963(95)00038-0.

Borcard D, Legendre P, Drapeau P. 1992. Partialling out the spatial component of ecological variation. *Ecology*, **73**(3): 1045-1055, https://doi.org/10.2307/1940179.

Chang F M, Zhuang L H, Li T G et al. 2003. Radiolarian fauna in surface sediments of the northeastern East China Sea. *Marine Micropaleontology*, **48**(3-4): 169-204, https://doi.org/10.1016/S0377-8398(03)00016-1.

Chen M H, Tan Z Y. 1996. Radiolaria from surface sediments of the central and northern South China Sea. Science Press, Beijing, China. 271p. (in Chinese)

Cheng X W, Zhang L L, Gao F et al. 2022. Biodiversity of zooplankton in 0-3000 m waters from the eastern Indian Ocean in spring 2019 based on metabarcoding. *Water Biology and Security*, **1**(1): 100005, https://doi.org/10.1016/j.watbs.2022.100005.

De Deckker P. 2016. The Indo-Pacific Warm Pool: critical to world oceanography and world climate. *Geoscience Letters*, **3**(1): 20, https://doi.org/10.1186/s40562-016-0054-3.

De Wever P, Dumitrica P, Caulet J P et al. 2001. Radiolarians in the Sedimentary Record. CRC Press, London. 533p, https://doi.org/10.1201/9781482283181.

Dworetzky B A, Morley J J. 1987. Vertical distribution of Radiolaria in the eastern equatorial Atlantic: analysis of a multiple series of closely-spaced plankton tows. *Marine Micropaleontology*, **12**: 1-19, https://doi.org/10.1016/0377-8398(87)90011-9.

Emery W J, Meincke J. 1986. Global water masses: summary and review. *Oceanologica Acta*, **9**(4): 383-391.

Feng Y F, Li J X, Yang S M. 2024. Response of phytoplankton communities to the physical processes of mesoscale eddy in the northern South China Sea in summer. *Advances in Marine Science*, **42**(4): 690-708, https://doi.org/10.12362/j.issn.1671-6647.20230306002. (in Chinese with English abstract)

Gaube P, McGillicuddy D J Jr, Moulin A J. 2019. Mesoscale eddies modulate mixed layer depth globally. *Geophysical Research Letters*, **46**(3): 1505-1512, https://doi.org/10.1029/2018GL080006.

Goll R M, Bjørklund K R. 1989. A new radiolarian biostratigraphy for the Neogene of the Norwegian Sea: ODP Leg 104. *In*: Eldholm O, Thiede J, Taylor E et al. eds. Proceedings of the Ocean Drilling Program, Scientific Results, vol 104. Texas A&M University, College Station, Texas. p.697-737.

Grand M M, Measures C I, Hatta M et al. 2015. Dissolved Fe and Al in the upper 1000 m of the eastern Indian Ocean: a high-resolution transect along 95°E from the Antarctic margin to the Bay of Bengal. *Global Biogeochemical Cycles*, **29**(3): 375-396, https://doi.org/10.1002/2014GB004920.

Haeckel E. 1887. Report on the Radiolaria collected by H. M. S. Challenger during the years 1873-1876. *Reports of Scientific Results*, *Challenger*, *Zoology*, **18**: 1-1803.

Han W Q, McCreary J P. 2001. Modeling salinity distributions in the Indian Ocean. *Journal of Geophysical Research*: *Oceans*, **106**(C1): 859-877, https://doi.org/10.1029/2000JC000316.

He Q Y, Zhan H G, Cai S Q. 2020. Anticyclonic eddies enhance the winter barrier layer and surface cooling in the Bay of Bengal. *Journal of Geophysical Research*:

Oceans, **125**(10): e2020JC016524, https://doi.org/10.1029/2020JC016524.

Hu W F, Zhang L L, Chen M H et al. 2015. Distribution of living radiolarians in spring in the South China Sea and its responses to environmental factors. *Science China Earth Sciences*, **58**(2): 270-285, https://doi.org/10.1007/s11430-014-4950-0.

Ikenoue T, Bjørklund K R, Fujiwara A et al. 2019. Horizontal and vertical distribution of polycystine radiolarians in the western Arctic Ocean during the late summers of 2013 and 2015. *Polar Biology*, **42**(2): 285-305, https://doi.org/10.1007/s00300-018-2421-3.

Ikenoue T, Bjørklund K R, Kruglikova S B et al. 2015. Flux variations and vertical distributions of siliceous Rhizaria (Radiolaria and Phaeodaria) in the western Arctic Ocean: indices of environmental changes. *Biogeosciences*, **12**(6): 2019-2046, https://doi.org/10.5194/bg-12-2019-2015.

Ishitani Y, Takahashi K. 2007. The vertical distribution of Radiolaria in the waters surrounding Japan. *Marine Micropaleontology*, **65**(3-4): 113-136, https://doi.org/10.1016/j.marmicro.2007.06.002.

Iskandar M R, Suga T. 2022. Change in salinity of Indonesian upper water in the southeastern Indian Ocean during Argo period. *Heliyon*, **8**(9): e10430, https://doi.org/10.1016/j.heliyon.2022.e10430.

Itaki T. 2003. Depth-related radiolarian assemblage in the water-column and surface sediments of the Japan Sea. *Marine Micropaleontology*, **47**(3-4): 253-270, https://doi.org/10.1016/S0377-8398(02)00119-6.

Itaki T, Ito M, Narita H et al. 2003. Depth distribution of radiolarians from the Chukchi and Beaufort Seas, western Arctic. *Deep Sea Research Part I*: *Oceanographic Research Papers*, **50**(12): 1507-1522, https://doi.org/10.1016/j.dsr.2003.09.003.

Jain V, Shankar D, Vinayachandran P N et al. 2017. Evidence for the existence of Persian Gulf water and Red Sea water in the Bay of Bengal. *Climate Dynamics*, **48**(9-10): 3207-3226, https://doi.org/10.1007/s00382-016-3259-4.

Jensen T G. 2003. Cross-equatorial pathways of salt and tracers from the northern Indian Ocean: modelling results. *Deep Sea Research Part II*: *Topical Studies in Oceanography*, **50**(12-13): 2111-2127, https://doi.org/10.1016/S0967-0645(03)00048-1.

Kling S A. 1979. Vertical distribution of polycystine radiolarians in the central North Pacific. *Marine Micropaleontology*, **4**: 295-318, https://doi.org/10.1016/0377-8398(79)90022-7.

Kling S A, Boltovskoy D. 1995. Radiolarian vertical distribution patterns across the southern California Current. *Deep Sea Research Part I*: *Oceanographic Research Papers*, **42**(2): 191-231, https://doi.org/10.1016/0967-0637(94)00038-T.

Kumar S P, Prasad T G. 1999. Formation and spreading of Arabian Sea high-salinity water mass. *Journal of Geophysical Research*: *Oceans*, **104**(C1): 1455-1464, https://doi.org/10.1029/1998JC900022.

Lampitt R S, Salter I, Johns D. 2009. Radiolaria: major exporters of organic carbon to the deep ocean. *Global Biogeochemical Cycles*, **23**(1): GB1010, https://doi.org/10.1029/2008GB003221.

Lazarus D B, Kotrc B, Wulf G et al. 2009. Radiolarians decreased silicification as an evolutionary response to reduced Cenozoic ocean silica availability. *Proceedings of the National Academy of Sciences of the United States of America*, **106**(23): 9333-9338, https://doi.org/10.1073/pnas.0812979106.

Lepš J, Šmilauer P. 2003. Multivariate Analysis of Ecological Data using CANOCO. Cambridge University Press, Cambridge. 269p., https://doi.org/10.1017/CBO9780511615146.

Llopis Monferrer N, Boltovskoy D, Tréguer P et al. 2020. Estimating biogenic silica production of Rhizaria in the global ocean. *Global Biogeochemical Cycles*, **34**(3): e2019GB006286, https://doi.org/10.1029/2019GB006286.

Lombari G, Lazarus D B. 1988. Neogene cycladophorid radiolarians from North Atlantic, Antarctic, and North Pacific deep-sea sediments. *Micropaleontology*, **34**(2): 97-135, https://doi.org/10.2307/1485657.

Lu M A. 1999. Paleoenvirnmental implication of Radiolaria in core NS93-5 from the sea areas of Nansha Islands. South China Sea Institute of Oceanology, Chinese Academy of Sciences, Guangzhou, China. p.2-3, http://doi.org/ir.scsio.ac.cn/handle/344004/3571. (in Chinese with English abstract)

Makarim S, Sprintall J, Liu Z Y et al. 2019. Previously unidentified Indonesian Throughflow pathways and freshening in the Indian Ocean during recent decades. *Scientific Reports*, **9**(1): 7364, https://doi.org/10.1038/s41598-019-43841-z.

Maldonado M, López-Acosta M, Sitjà C et al. 2019. Sponge skeletons as an important sink of silicon in the global oceans. *Nature Geoscience*, **12**(10): 815-822, https://doi.org/10.1038/s41561-019-0430-7.

Matsuoka A, Anderson O R. 1992. Experimental and observational studies of radiolarian physiological ecology: 5. Temperature and salinity tolerance of *Dictyocoryne truncatum*. *Marine Micropaleontology*, **19**(4): 299-313, https://doi.org/10.1016/0377-8398(92)90035-I.

Matsuzaki K M, Itaki T, Kimoto K. 2016. Vertical distribution of polycystine radiolarians in the northern East China Sea. *Marine Micropaleontology*, **125**: 66-84, https://doi.org/10.1016/j.marmicro.2016.03.004.

Matsuzaki K M, Itaki T, Sugisaki S. 2020. Polycystine radiolarians vertical distribution in the subtropical Northwest Pacific during Spring 2015 (KS15-4). *Paleontological Research*, **24**(2): 113-133, https://doi.org/10.2517/2019PR019.

McMillen K J, Casey R E. 1978. Distribution of living polycystine radiolarians in the Gulf of Mexico and Caribbean Sea, and comparison with the sedimentary record. *Marine Micropaleontology*, **3**(2): 121-145, https://doi.org/10.1016/0377-8398(78)90002-6.

McNaughton S J. 1967. Relationships among functional properties of Californian grassland. *Nature*, **216**(5111): 168-169, https://doi.org/10.1038/216168b0.

Munir S, Rogers J, Zhang X D et al. 2020. The horizontal distribution of siliceous planktonic radiolarian community in the eastern Indian Ocean. *Water*, **12**(12): 3502, https://doi.org/10.3390/w12123502.

Munir S, Sun J, Morton S L. 2021. The first record and classification of planktonic radiolarian (*Phylum Retaria*) and phaeodarian (*Phylum Cercozoa*) in the Eastern Indian Ocean. *Biology*, **10**(3): 202, https://doi.org/10.

3390/biology10030202.

Okazaki Y, Takahashi K, Itaki T et al. 2004. Comparison of radiolarian vertical distributions in the Okhotsk Sea near the Kuril Islands and in the northwestern North Pacific off Hokkaido Island. *Marine Micropaleontology*, **51**(3-4): 257-284, https://doi.org/10.1016/j.marmicro.2004.01.003.

Priyanka K, Sarangi R K, Poornima D et al. 2025. Development of new production algorithm in the northern Indian Ocean and observation of enhanced productivity using satellite remote sensing. *Discover Oceans*, **2**(1): 8, https://doi.org/10.1007/s44289-025-00044-x.

Qiu Z Y, Zhang L L, Xiang R et al. 2021. Biodiversity of radiolarians in surface sediments from the East Indian Ocean and their implication for water masses. *Deep Sea Research Part I*: *Oceanographic Research Papers*, **177**: 103625, https://doi.org/10.1016/j.dsr.2021.103625.

Qiu Z Y, Zhang L L, Yang Y P et al. 2024. Significant terrigenous dilution affected biogenic deposits in the Bay of Bengal during the last deglaciation to glaciation. *Global and Planetary Change*, **238**: 104477, https://doi.org/10.1016/j.gloplacha.2024.104477.

Renz G W. 1976. The Distribution and Ecology of Radiolaria in the Central Pacific: Plankton and Surface Sediments. University of California Press, Berkeley. 267p.

Rixen T, Ittekkot V. 2005. Nitrogen deficits in the Arabian Sea, implications from a three component mixing analysis. *Deep Sea Research Part II*: *Topical Studies in Oceanography*, **52**(14-15): 1879-1891, https://doi.org/10.1016/j.dsr2.2005.06.007.

Rochford D J. 1964. Salinity maxima in the upper 1000 metres of the North Indian Ocean. *Marine and Freshwater Research*, **15**(1): 1-24, https://doi.org/10.1071/mf9640001.

Schott F A, McCreary J P Jr. 2001. The monsoon circulation of the Indian Ocean. *Progress in Oceanography*, **51**(1): 1-123, https://doi.org/10.1016/S0079-6611(01)00083-0.

Sheehan P M F, Webber B G M, Sanchez-Franks A et al. 2020. Injection of oxygenated Persian Gulf water into the Southern Bay of Bengal. *Geophysical Research Letters*, **47**(14): e2020GL087773, https://doi.org/10.1029/2020GL087773.

Sloyan B M. 2006. Antarctic bottom and lower circumpolar deep water circulation in the eastern Indian Ocean. *Journal of Geophysical Research*: *Oceans*, **111**(C2): 2005JC003011, https://doi.org/10.1029/2005JC003011.

Suzuki N, Not F. 2015. Biology and ecology of radiolaria. *In*: Ohtsuka S, Suzaki T, Horiguchi T et al. eds. Marine Protists. Springer, Tokyo, Japan. p.179-222, https://doi.org/10.1007/978-4-431-55130-0_8.

Takahashi K. 1991. Mineral flux and biogeochemical cycles of marine planktonic protozoa—session summary. *In*: Reid P C, Turley C M, Burkill P H eds. Protozoa and Their Role in Marine Processes. Springer, Berlin, Germany. p.347-359, https://doi.org/10.1007/978-3-642-73181-5_21.

Talley L D, Sprintall J. 2005. Deep expression of the Indonesian throughflow: Indonesian intermediate water in the south equatorial current. *Journal of Geophysical Research*: *Oceans*, **110**(C10): C10009, https://doi.org/10.1029/2004JC002826.

Tanaka S, Takahashi K. 2008. Detailed vertical distribution of radiolarian assemblage (0-3000 m, fifteen layers) in the central subarctic Pacific, June 2006. *Memoirs of the Faculty of Science*, *Kyushu University. Series D*, *Earth and Planetary Sciences*, **32**(1): 49-72, https://doi.org/10.5109/11807.

Verma S, Gupta A K, Singh R K. 2013. Variations in deep-sea benthic foraminifera at ODP Hole 756B, southeastern Indian Ocean: evidence for changes in deep ocean circulation. *Palaeogeography*, *Palaeoclimatology*, *Palaeoecology*, **376**: 172-183, https://doi.org/10.1016/j.palaeo.2013.02.034.

Welling L A, Pisias N G, Johnson E S et al. 1996. Distribution of polycystine radiolaria and their relation to the physical environment during the 1992 El Niño and following cold event. *Deep Sea Research Part II*: *Topical Studies in Oceanography*, **43**(4-6): 1413-1434, https://doi.org/10.1016/0967-0645(96)00013-6.

Wyrtki K. 1973. Physical oceanography of the Indian Ocean. *In*: Zeitzschel B, Gerlach S A eds. The Biology of the Indian Ocean. Springer, Berlin, Germany. p.18-36, https://doi.org/10.1007/978-3-642-65468-8_3.

Yasuda I, Kouketsu S, Katsumata K et al. 2002. Influence of okhotsk sea intermediate water on the oyashio and north pacific intermediate water. *Journal of Geophysical Research*: *Oceans*, **107**(C12): 3237, https://doi.org/10.1029/2001jc001037.

You Y, Tomczak M. 1993. Thermocline circulation and ventilation in the Indian Ocean derived from water mass analysis. *Deep Sea Research Part I*: *Oceanographic Research Papers*, **40**(1): 13-56, https://doi.org/10.1016/0967-0637(93)90052-5.

You Y Z. 1997. Seasonal variations of thermocline circulation and ventilation in the Indian Ocean. *Journal of Geophysical Research*: *Oceans*, **102**(C5): 10391-10422, https://doi.org/10.1029/96JC03600.

Zasko D N, Rusanov I I. 2005. Vertical distribution of radiolarians and their role in epipelagic communities of the east Pacific Rise and the Gulf of California. *Biology Bulletin*, **32**(3): 279-287, https://doi.org/10.1007/s10525-005-0103-5.

Zhang J, Zhang L L, Xiang R et al. 2020. Radiolarian biogeographic contrast between spring of 2017 and winter of 2017-2018 in the South China Sea and Malacca Strait. *Continental Shelf Research*, **208**: 104245, https://doi.org/10.1016/j.csr.2020.104245.

Zhang L L, Chen M H, Xiang R et al. 2009. Distribution of polycystine radiolarians in the northern South China Sea in September 2005. *Marine Micropaleontology*, **70**(1-2): 20-38, https://doi.org/10.1016/j.marmicro.2008.10.002.

Zhang L L, Cheng X W, Xiang R et al. 2023. Changes of radiolarian community structure with depth in the central Bay of Bengal in spring 2019. *Journal of Tropical Oceanography*, **42**(4): 166-175, https://doi.org/10.11978/2022209. (in Chinese with English abstract)

Zhang L L, Suzuki N, Nakamura Y et al. 2018. Modern shallow water radiolarians with photosynthetic microbiota in the western North Pacific. *Marine Micropaleontology*, **139**: 1-27, https://doi.org/10.1016/j.marmicro.2017.10.007.

Zhang L L, Wang R J, Chen M H et al. 2015. Biogenic silica in surface sediments of the South China Sea: controlling factors and paleoenvironmental implications. *Deep Sea Research Part II*: *Topical Studies in Oceanography*, **122**: 142-152, https://doi.org/10.1016/j.dsr2.2015.11.008.